The Abdus Salam
International Centre for Theoretical Physics

United Nations
Educational, Scientific and
Cultural Organization

IAEA
International Atomic Energy Agency

2152-7

Joint ICTP-IAEA Course on Natural Circulation Phenomena and Passive Safety Systems in Advanced Water Cooled Reactors

17 - 21 May 2010

INSIGHTS INTO NATURAL CIRCULATION STABILITY

F. D'Auria, A. Del Nevo and N. Muellner

University of Pisa
DIMNP
Italy

University of Vienna
IRF
Wien
Austria

IAEA Course on Natural Circulation
ICTP, Trieste, Italy
May 17-21, 2010, Paper ID T-7

INSIGHTS INTO NATURAL CIRCULATION STABILITY - UPDATED

F. D'Auria [1], A. Del Nevo [2], N. Muellner [3]

1: University of Pisa, DIMNP, Pisa, Italy, dauria@ing.unipi.it
2: University of Pisa, DIMNP, Pisa, Italy, , a.delnevo@ing.unipi.it
3: University of Vienna, IRF, Wien, Austria nikolaus.muellner@univie.ac.at

KEY WORDS

Natural circulation, Instability, Fundamentals, Reliability of natural circulation phenomenon.

LECTURE OBJECTIVES

The scholar will understand the meaning and the importance of stability in fluid-dynamics and mainly in natural circulation conditions. The scholar shall be able to perform the design of a natural circulation system accounting for stability, namely providing that the system is stable and, possibly, far from stability boundaries for the various conditions foreseen within the operational life.

1. INTRODUCTION

Stability of natural circulation flow is very challenging for scientists and investigators and of utmost importance for industrial applications. What means 'stability' within the context of natural circulation? One intuitive definition can be taken from Misale et al. (1999). <<*If the flow of the system in question (a simple loop, the atmosphere, a nuclear reactor, etc.) is stationary in respect to the temperature, and the velocity, it can be called "stable". If the flow and the temperature show some oscillations, but the amplitude of the oscillations and the sign of the velocity stay constant in time, the system can be called "neutral". If, finally, the system shows oscillations which grow in time and lead to flow reversal, the system can be called "unstable"*>>.

Why is it useful to still study instability? This question is best answered by pointing out the wide range of applications. Natural circulation phenomena are utilized in areas like solar heaters, geothermal energy production, space travel, cooling of engines, and of course for cooling nuclear reactors. Some reactors and reactor designs also utilize natural circulation primary source for the heat transfer during normal operation, like the Dodewaard reactor in Netherlands (shutdown in 1999 following around 30 years of operation). It is obvious that for applications like this the engineer must have the theoretical tools available to study the regions of stability and instability and must have knowledge which parameters will influence the behavior of the system.

This lecture aims at providing an overview over stability in natural circulation. Relevant definitions are introduced together with the presentation of different kinds of instability modes and of parameters which influence the stability. Reference is made to recent developments in the field. A top-down approach is pursued. In the first part of the paper data measured in a complex (Boiling Water Reactor) and in a simple (rectangular loop for space applications) natural circulation system are provided to show the features of single and two-phase thermal-hydraulic instabilities: Furthermore, the objectives and the results of a reliability study for passive systems are discussed to show the industrial relevance of the stability. In the second part of the paper, theoretical models are presented for the simulation of unstable systems and, in general, aimed at the solution of stability problems.

1.1 The LaSalle Event

On March 9 1988, the unit 2 of LaSalle Nuclear Power Plant (NPP) underwent a dual recirculation pump trip, following which the unit experienced excessive neutron flux oscillations while it was in natural circulation (Ambrosini et al., 1995). LaSalle-2 is a 930 MWe BWR designed by General Electric.

The unit had been operating at 84% power with 76% flow when an instrument technician, performing surveillance on the initiation logic for the reactor core isolation cooling, opened a wrong valve. The resulting perturbation on the switches for anticipated transient without scram resulted in a trip of both recirculation pumps. This caused a reduction in flow from forced to natural circulation, while the control rods remained in the 99% flow control line position. The resultant power-to-flow condition (about 40% power with natural circulation, i.e. around 30% core flow) after the pump trip was known to be a condition susceptible to instability. In addition, as a result of the rapid power reduction due to the loss of the recirculation pumps, there was a perturbation in the feed-water heaters causing a loss of various feed-water pre-heaters. This resulted in an insertion of positive reactivity as cooler feed-water was supplied to the reactor. The net effect was an increase in power that further reduced the margin to instability. Approximately 5 minutes after the recirculation pump trip, the operators noted that the Average Power Range Monitor (APRM) indications were oscillating between 25 and 50% power every 2 to 3 seconds, and the Local Power Range Monitor (LPRM) alarms began to annunciate and clear. The operators unsuccessfully attempted to restart the recirculation pumps to re-establish the forced flow. Nearly 7 minutes after the pump trip, another attempt to restore the forced flow was unsuccessful and, while operators were preparing for a manual scram, the reactor automatically scrammed on high flux (118% trip). The plant was taken to cold shutdown. The oscillations were “in-phase”.

A picture of the plant performance before the power excursion that caused the scram, can be derived from Fig. 1. Power oscillations in NC conditions, measured by three APRM systems, having the typical 0.5 Hz frequency, can be noted.

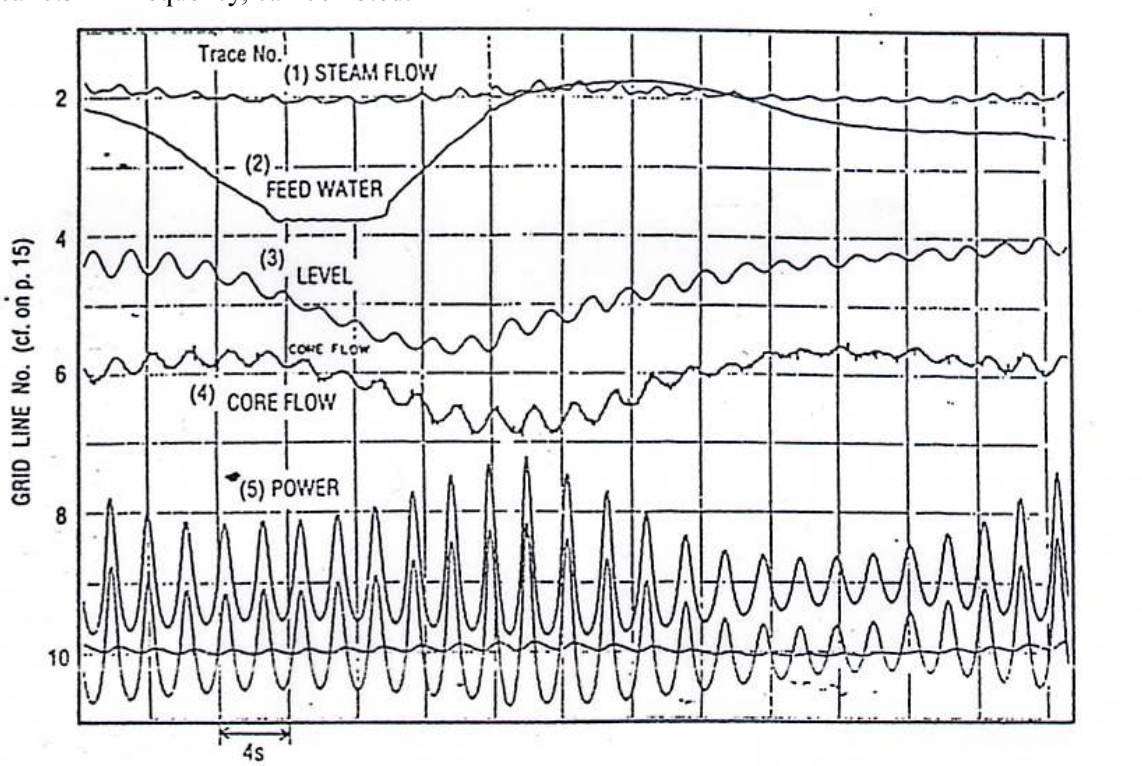

FIG. 1. Natural Circulation stability in a (BWR) complex system: LaSalle-2 NPP event, 1988, available plant measurements from STARTREC (STARtup Transient data RECorder) system.

1.2 Instability in a loop

An experimental research has been completed in relation to the possibility to design a natural circulation system in the absence of gravity (or in microgravity conditions), Fig. 2.

a)

b)

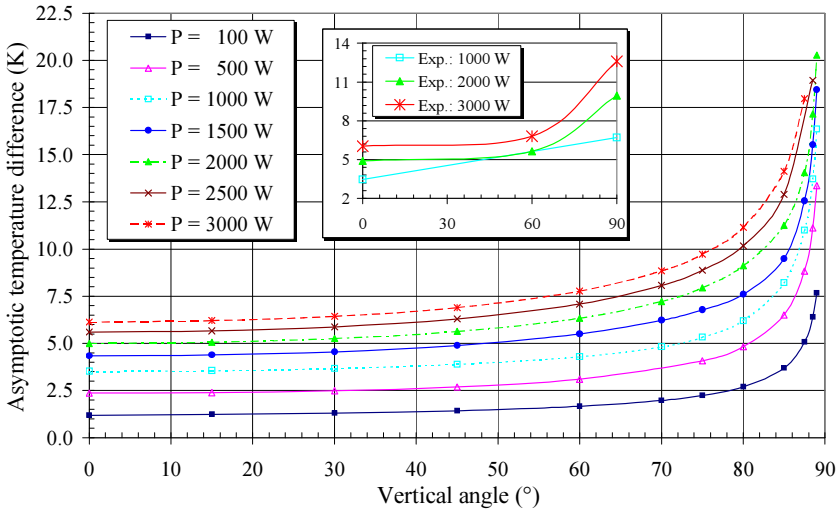

c)

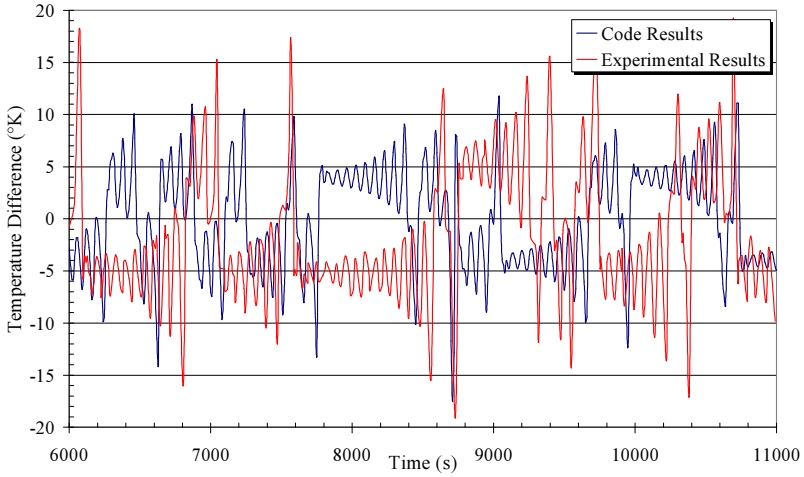

FIG. 2. Natural Circulation stability in a simple system, space application: a) picture of the loop installed in movable frame; b) measured temperature difference across the heater when the angle of the frame is varied; c) typical oscillations measured and calculated for the vertical position of the frame ('0' vertical angle).

To this aim Petruzzi et al., (2002) installed a NC rectangular loop (heater and cooler in the bottom and in the top horizontal legs, respectively) on a rotating frame, Fig. 2a: when the loop is in the vertical position the gravitational forces drive the natural circulation phenomena; the same force reduces to (nearly) 'zero' when the supporting frame is rotated to the horizontal position. Natural circulation flow-rates as a function of the gravity angle can be deduced from the diagram in Fig. 2b (the '0' and the '90' angles corresponds to vertical and the horizontal plane, respectively). Instability remains a problem for any angle of the frame as depicted in Fig. 2c (Petruzzi et al., 2001).

1.3 Reliability evaluation of a NC System

J. Jafari et al. (2003) investigated the reliability of a natural circulation system, namely the TTL-1 loop, working in single and two-phase conditions, Fig. 3. The term reliability (of a passive system), within the context of NC was defined first and failure criteria for the loop performance were fixed. Loop design parameters affecting the transient NC performance were selected with related variation ranges. The loop model suitable by a thermal-hydraulic code was built and care was taken in demonstrating the compliance of code results with experimental. Then, around one hundred calculations by the qualified code-model were run with results from about twenty of the calculations shown in Fig. 3a).

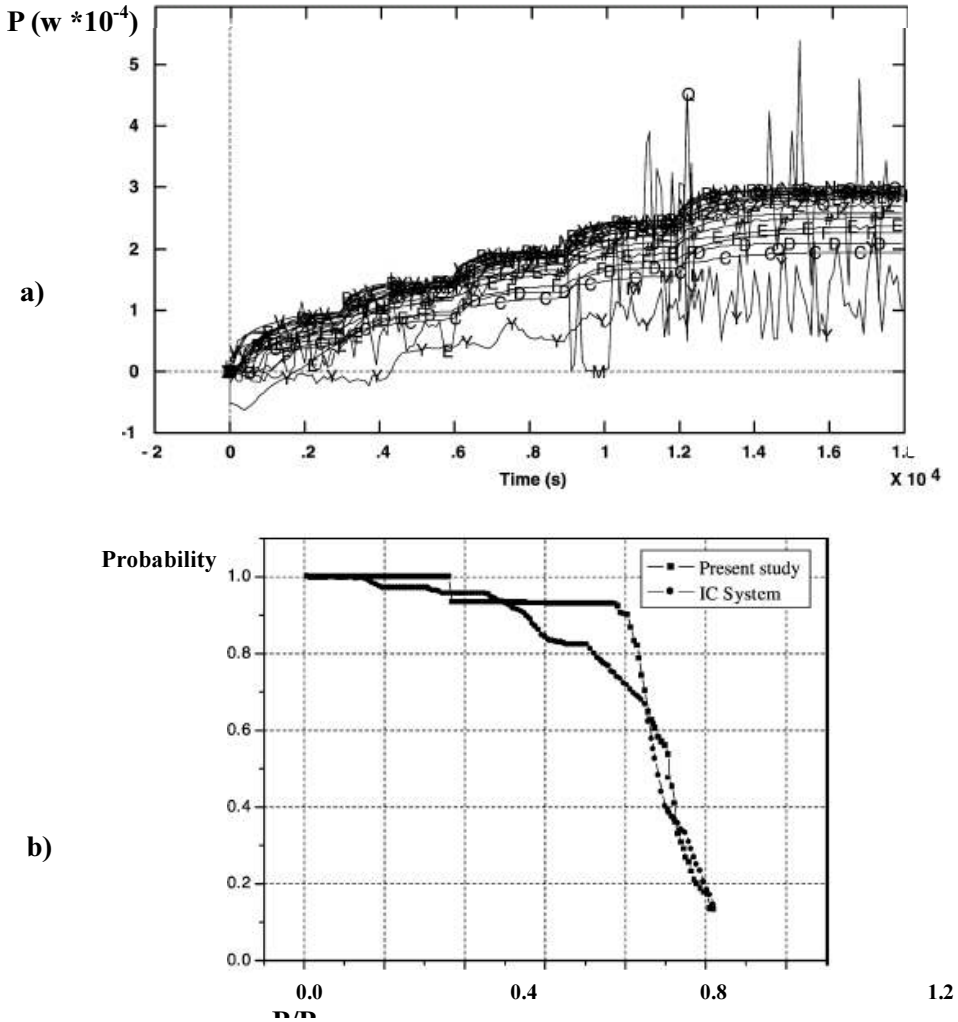

FIG. 3. Reliability of the TTL-1 natural circulation system: a) power exchanged in the cooler as a function of time in different design conditions; b) reliability of TTL-1 NC system <present study> and comparison with the results from the analysis of a different NC system.

The comparison between the target power transferred from the heater to the cooler (e.g. failure criteria above) and the actual power (e.g. diagram in Fig. 3a), constituted the basis for evaluating the reliability of the NC system (TTL-1 loop). The results, reported in Fig. 3b in terms of failure probability versus the 'amount of failure' (indicated by the ratio "power exchanged / target power") show that the instability is the key factor in causing system unreliability.

2. FUNDAMENTALS

2.1 Definition of stability in fluid dynamics

It seems worthwhile to introduce hereafter some definitions that are common to the stability analyses in fluid-dynamics, see also D'Auria et al. 1997.

- **Acoustic instability**: this occurs when standing waves are excited in a single or two phase system with a frequency in the acoustic range (steam line resonance and acoustic instabilities in the steam dome and upper plenum regions of BWR have been observed).

- **Decay ratio**: the DR is defined as the ratio of two consecutive maxima of the impulse response. Two methods for extracting the DR value from neutron noise signal are commonly in use: a) utilizing the autocorrelation function ; b) from the impulse response which can be obtain by autoregressive modeling of the neutron noise. Either A1/A2 (ratio of two consecutive maxima related to the horizontal time axis) either B1/B2 (ratio of distances between two consecutive peaks and a line connecting the "opposite peaks") can be taken to obtain the DR value.

- **Density wave**: a density wave is a perturbation in the density of the fluid mixture, which travels along the heated channel with a characteristic speed depending on local conditions. Density wave oscillations (DWO) are the basic mechanism credited for triggering and sustaining the relevant oscillation phenomena in boiling water reactor cores. In other words, the observed instability phenomena have been explained making reference to the delays involved in density wave propagation.

- **Dynamic instabilities**: these terms characterize the wider class of instabilities that can be studied only through the use of time-dependent balance equations.

- **Flow excursion (Ledinegg) instability**: this is a type of static instability that is determined by the relationship between the pressure drop characteristic of a boiling channel and the pressure drop characteristic imposed by an external system.

- **Flow regime induced instability**: the periodicity of some flow regime (e.g. slug flow) excite this instability mode.

- **Flow regime "relaxation" instability**: this is a static instability due to flow regime changes.

- **Limit cycle**: limit cycle is a particular long term periodic solution of the differential equations describing a non-linear system, which is encountered studying the system behavior beyond the linear stability threshold. Limit cycles are named "stable", if they attract system trajectories starting from nearby states, or "unstable", if they repel them. Stable limit cycles have been observed in BWR and other boiling systems during instabilities and are ideally characterized by a periodic oscillatory behavior with constant amplitude and frequency. As a matter of fact, limit cycles observed in BWR during tests or inadvertent occurrences are not so ideal, showing gradual changes in amplitude and frequency of oscillations as a result of drift in system parameters.

• **Pressure drop oscillations (PDO)**: in this case a Ledinegg type instability and a compressible volume in the boiling system interact. It might be noted that PDO is a dynamic type of oscillations and Ledinegg is a static one.

• **Stability boundary**: A stability boundary is represented by a relationship between the parameters describing a system status which defines the conditions in which the system shows marginal (or neutral) stability, i.e. in which perturbations are neither amplified nor damped. In a two-dimensional parameter space, this relationship can be represented as a curve separating areas of stable and unstable behavior. Hyper-surfaces separating stable and unstable multidimensional domains are obtained in the case of systems described by several parameters.

• **Stability margin**: a stability margin is a properly defined measure of the distance of a system status from the stability boundary. For instance, control theory suggests the use of "gain" and "phase" margins as a measure of the stability of a linear system.

• **Static instability**: these terms identify a class of instabilities that can be theoretically explained without the use of time-dependent conservation equations.

• **Thermal-hydraulic instabilities**: These are identified by periodic time oscillations of various quantities in a boiling system (either single channel either parallel channels). Excursion of heated wall surface temperature may result from thermal-hydraulic instabilities. This includes the entire class of instabilities discussed.

• **Thermal oscillations**: Are oscillations heavily involving the heater dynamics in a boiling channel. Cyclic dry-out and rewet phenomena may be involved at a frequency lower than DWO.

2.2 Relevant stability related parameters

A classification of the thermal-hydraulic instabilities, summarized in table 1, can be explained considering two main groups: the so-called 'static' instabilities, that are explainable in terms of steady state laws, and the 'dynamic' instabilities, that requires the use of the time dependent conservation equations and, in case, the adoption of concepts and techniques developed in the frame of control theory.

Parameters through which stability shows up (flow rate, pressure, density, temperature)

LEDINEGG INSTABILITIES
Ledinegg instabilities are due to the particular S-shape that the flow rate versus pressure drop characteristic of a boiling channel often exhibits, Fig. 4. The analyses performed in a simplified loop (representing an helical coil steam generator) has shown that the effect of the energy loss coefficient in the two-phase zone has a destabilizing effect, while the large inlet pressure drop due to orifice has a general stabilizing effect against the "Ledinegg" instability (Ambrosini et al., 2004).

FUNDAMENTAL RELAXATION INSTABILITY
Flow pattern transition instabilities have been postulated as occurring when the flow conditions are close to the point of transition between bubbly flow and annular flow. A temporary reduction in flow rate may cause the increase of the bubble population and the change of the flow pattern to annular flow (characterized by low pressure drop). The consequence is that with the flow rate increase, the vapor generated is not sufficient to maintain the annular flow and the flow pattern then reverts to that of the bubbly-slug flow. The cycle can be repeated. Length, inlet temperature, mass velocity, and pressure are related to the large scale fluctuations characteristic of the slug flow regime that can be viewed as a transition from bubbly to annular flow, in particular related to a low pressure diabatic flow (Boure, 1973).

TABLE 1. CLASSIFICATION OF FLOW INSTABILITIES

Class	Type	Mechanism	Characteristic
Static instabilities			
Fundamental (or pure) static instabilities	Flow excursion or Ledinegg instabilities	$\left.\frac{\partial \Delta p}{\partial G}\right\|_{int} \leq \left.\frac{\partial \Delta p}{\partial G}\right\|_{ext}$	Flow undergoes sudden, large amplitude excursion to a new, stable condition
	Boiling crisis	Ineffective removal of heat from heated surface	Wall temperature excursion and flow oscillation
Fundamental relaxation instability	Flow pattern transition instability	Bubbly flow has less void but higher ΔP than that of annular flow	Cyclic flow pattern transitions and flow rate variations
Compound relaxation instability	Bumping, geysering, or chugging	Periodic adjustment of metastable condition, usually due to lack of nucleation sites	Period process of super-heat and violent evaporation with possible expulsion and refilling
Dynamic instabilities			
Fundamental (or pure) dynamic instabilities	Acoustic oscillations	Resonance of pressure waves	High frequencies (10-100 Hz) related to the time required for pressure wave propagation in system
	Density wave oscillations	Delay and feedback effects in relationship between flow rate, density, and pressure drop	Low frequencies (1 Hz) related to transit time of a continuity wave
Compound dynamic instabilities	Thermal oscillations	Interaction of variable heat transfer coefficient with flow dynamics	Occurs in film boiling
	BWR instability	Interaction of void reactivity coupling with flow dynamics and heat transfer	Strong only for small fuel time constant and under low pressures
	Parallel channel instability	Interaction among small number of parallel channels	Various modes of flow redistribution
Compound dynamic instability as secondary phenomena	Pressure drop oscillations	Flow excursion initiates dynamic interaction between channel and compressible volume	Very low frequency periodic process (0.1 Hz)

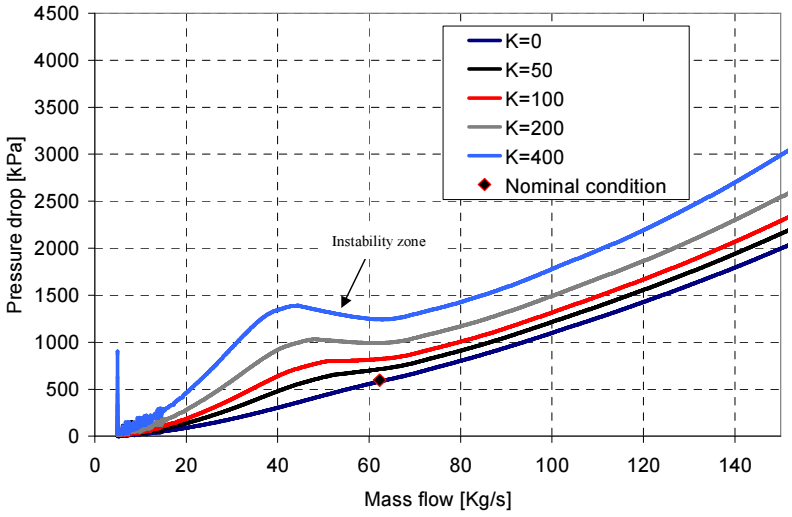

FIG. 4. Calculation of the static SG characteristics with Relap5 code; effect of the energy loss coefficient (in two phase zone) on the pressure drop characteristic.

COMPOUND RELAXATION INSTABILITY

Bumping, geysering and chugging involve static phenomena which are coupled so as to produce a repetitive behavior which is not necessarily periodic.

Bumping is exhibited in boiling of the alkali metals at low pressure. It has been postulated that it is due to the presence of gas in certain cavities.

Geysering has been observed in a variety of closed end, vertical columns of liquid which are heated at the base. In low pressure systems this is suddenly increased vapor generation due to reduction in hydrostatic head, and usually an expulsion of vapor from the channel. The liquid then returns, the sub-cooled non-boiling condition is restored, and the cycle starts over again.

The term chugging is usually reserved for the cycle phenomenon characterized by a periodic expulsion of coolant from the flow channel. The expulsion may range from simple transitory variations of the inlet and outlet flow rates to violent ejections of coolant, usually through both ends of the channel (Boure, 1973). It may be noted that the term chugging is also used to characterize the pressure and flow oscillations that may occur following the blow-down period in a Pressure Suppression Pool (PSP) type of containment. In the PSP systems, typically adopted for BWR, the air present in the drywell is discharged into the wet-well free space passing through the liquid pool. At some time during the transient (i.e. a few tens of seconds after the transient start in case of large break LOCA), only two-phase steam-liquid mixture is present in the dry-well and all the non-condensable gas is accumulated in the wet-well. At this time, also triggered by pressure oscillations caused by steam condensing in the pool, a sudden steam condensation may occur in the drywell that causes large amplitude oscillation and consequent flow reversal from wet-well to dry-well and mechanical loads on the walls separating wet-well and dry-well.

DENSITY WAVE OSCILLATION (DWO)

Density-wave oscillations occur on the boiling positive slope branch of the pressure drop versus flow rate curve. Disturbances in gas-liquid two phase flows may be transported by different mechanisms among which are density wave resulting from fluctuations in void fraction (DWO), P. Carey, 1992.

DWO are most often observed in flow boiling processes in which the flow enters as sub-cooled liquid. The time scale associated with DWO is about the time required for a fluid particle to travel through the channel. The relevance of this phenomenon is due to the possibility that it could affect the operation and the safety characteristics of the system. DWO may cause undesired problems such as mechanical and thermal fatigue damage of the components through the mechanical vibration and thermal wave. The DWO and their consequences require proper attention at the level of system design, e.g. Guanghui et al., 2001, Kakac et al., 1991.

The main parameters that influence the DWO are Crowley et al., 1969, and Ishii, 1976.

- Increase in mass flow rate increases stability.
- Increase in heater power decreases stability.
- Increase in overall density ratio decreases stability.
- Increase in power input to the channel increases frequency.
- Increase of inlet sub-cooling increases stability at high sub-cooling.
- Increase in system pressure for a given power input increases stability.
- Decrease of the heated length increases the flow stability in forced.

PRESSURE DROP OSCILLATION (PDO)

Pressure-drop oscillations occur on the negative slope branch of the pressure drop versus flow rate curves. The name is referred to flow oscillations due to a multi-valued (S-shape) flow rate versus pressure drop characteristic. Flow oscillations, rather then one time excursion, can occur if there are a

sufficient interaction and delay feedbacks between flow rate and mass accumulation (i.e. compressibility) in the heated section or in the system. The required compressible volume may be situated outside the heated section or can be provided by the internal compressibility of long heated sections. Parameter effects connected with PDO can be summarized as follows, e.g. Yadigaroglu and Chan 1979:

- Increase in negative slope decreases stability.
- Increase in heater power decreases stability.
- Increase in exit pressure drop decreases stability.
- Increase in inlet pressure drop decreases stability.
- Period of pressure-drop oscillations increases with decrease in flow rate.
- Superimposed density-wave oscillations appear on low flow part of the pressure-drop type oscillation cycle.
- Boiling upward flows are more stable than horizontal flows.

THERMAL HYDRAULIC OSCILLATION (THO)

Thermal oscillations occur in a domain located within density-wave and pressure-drop oscillation regions where there is film boiling. During part of the cycle there are always superimposed density-wave oscillations. Typically, both the period and the amplitude are nearly inversely proportional to inlet mass flow rate. Additional parameter effects associated with THO can be summarized as follows, e.g. D'Auria et al. 1997:

- The amplitude increases with heat input, and the period increases linearly with heat input.
- In certain operation regions, both the period and the amplitude increase with decreasing inlet liquid temperature.
- Increase in inlet pressure drop increases stability.

Parameters affecting stability – mechanical and heat transfer interactions

Parameters which affect stability in natural circulations and were not mentioned above are mainly mechanical interactions and heat transfer interactions. Mechanical interactions comprise for example the propagation of pressure waves through the piping caused by the rapid closure of a valve (water-hammer). Mechanical interactions which are affecting stability are beyond the scope of this lecture and are only mentioned for completeness.

The influence of the thermal properties of the materials on the stability has been studied by M. Misale et al., 1999. A rectangular natural circulation loop was considered (i.e. the "Welander problem" discussed in detail in chapter 3). A natural circulation loop is a simple rectangular loop of pipes, which is subjected to gravity, heated at the bottom and cooled at the top. The fluid in the loop will be heated at the bottom, expand, and due to the buoyancy rise to the top, where it will be cooled again and will sink to the bottom. By this, natural circulation is established. The first one who presented an analysis of this problem was Welander, 1967.

As will be shown later, even a simple system as just described can show regions of instability. Even more surprisingly, the regions of stability and the behavior of the loop depend on the heat capacity of the piping which was demonstrated numerically by the cited paper (Misale et al., 1999, see also D'Auria et al. 1997a and Frogheri et al., 1998) and experimentally by Vijayan and Austregesilo, 1994. The data reported in Tab. 2, Misale et al. 1999, are the results of three different series of simulations where the piper thermal capacity has been changed. The thermal capacity is assumed equal in all the pipes that constitute the three considered loops that are different due to materials: copper, steel and plexiglas, respectively. The influence of the thermal capacity can be noticed from the Reynolds number. If the thermal capacity (and the conductivity) of the hot section pipe decreases, e.g. when changing material from copper to plexiglas, at constant heat flux, the average temperature of the pipe

increases and a higher buoyancy force is established in the fluid. The loop considered in Tab. 2 is the same loop shown in Fig. 2a), and other than the standard symbolisms used for non dimensional groups (i.e. Reynolds, Prandtl and Nusselt numbers), 'f' is the friction coefficient.

TABLE 2. THE DIFFERENT BEHAVIOR OF THE NC LOOP PREDICTED WITH THREE DIFFERENT PIPING MATERIALS

	Heat flux (w)	**100**	**150**	**200**	**250**
Copper	Nu	8.8	10.1	11.1	11.9
	Re	342	452	559	664
	Pr	8.2	7.9	7.7	7.5
	fRe	20.8	23.2	25.1	26.6
Steel	Nu	9.1	10.4	11.4	12.3
	Re	347	461	571	680
	Pr	8.2	7.9	7.6	7.4
	fRe	20.9	23.3	25.1	26.6
Plexiglass	Nu	13.2	15.4	16.9	18.1
	Re	563	865	1219	1622
	Pr	6.8	6.0	5.4	4.8
	fRe	24.6	28.1	30.9	33.1

3. THE SINGLE PHASE STABILITY: THE WELANDER PROBLEM

In 1967 Pierre Welander (Welander, 1967) published a paper in the Journal of Fluid Mechanics about a surprisingly simple problem, which still keeps the scientific community interested. Consider a closed loop, subjected to gravity, which is heated at the bottom and cooled at the top, Fig. 5. The vertical tubes of the loop are insulated, the diameter of the loop is the same over the whole loop. The fluid motion will be driven by the buoyancy force, eq. (1): the fluid will heat up at the bottom, expand with the expansion coefficient α and will be driven to the top due to gravity, where it will be cooled again. The motion is affected by frictional forces. Welander assumed that in first approximation frictional forces are linear related to the flow eq. (2).

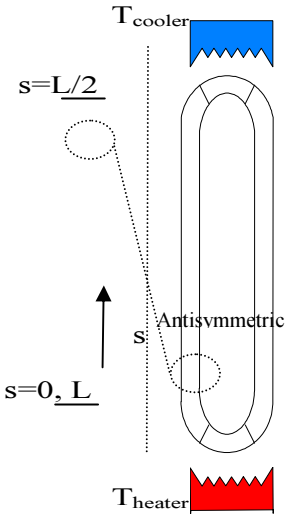

A point heat source and sink are assumed – this means that the heat transfer coefficient k tends towards infinity while the heated length Δs tends towards zero. The product k Δs stays finite (which is a boundary condition). The point of origin of the temperature is chosen to be the mean of T_{COOLER} and T_{HEATER}, so that

$$T_{HEATER} = -T_{COOLER}$$

The following assumptions are made:

1. ***the Boussinesq approximation is valid;***
2. ***the wall friction force on the fluid is proportional to the instantaneous flow rate q;***
3. ***the temperature of the fluid is uniform over each cross-section;***
4. ***the heat flux between the fluid is uniform over each cross section.***

An anti-symmetric initial temperature distribution is assumed (anti-symmetric with respect to the center of the loop). This is physically plausible and can be shown that the anti-symmetry is preserved over the time. Therefore it is possible to restrict the analysis to one half of the loop.

FIG. 5. A simple closed loop with a heater at the bottom and a heat sink at the top. It is filled with liquid in sub-cooled conditions

The Welander equations are (symbols provided at the end of the document):

(1) $\overline{B} = Ag\rho_0\alpha\oint Tdz$

(2) $\overline{F} \propto q$

If the equations (1) and (2) are used, the equation of motion can be written as:

(3) $\dot{q} = \frac{A}{L} g\alpha\oint Tdz - Rq$

For the heat transfer from the point source and sink to the fluid the model-assumptions defined by eq. (4) are used. Welander assumes that the increase (decrease) in temperature of the fluid when the fluid passes the heat source (sink) is proportional to the difference between the heater temperature and the fluid upstream of the heater. The factor ($1\text{-}e^{k\Delta t}$) accounts for the time in which the fluid passes the heater. If the fluid velocity is high the factor will be close to zero and T_{OUT} will be almost equal to T_{IN}. On the other hand, if the fluid velocity is small, the factor will be close to one and T_{OUT} will be almost equal to T_{HEATER}.

(4) $T_{OUT} - T_{IN} = \left(T_{HEATER} - T_{IN}\right)\cdot\left(1 - e^{k\Delta t}\right) = \left(T_{HEATER} - T_{IN}\right)\cdot\left(1 - e^{\frac{kA\Delta s}{|q|}}\right)$

Dimensionless coordinates were introduced (5).

(5) $s = \bar{s}\frac{L}{2},\ \ t = \bar{t}\frac{L}{2k\Delta s},\ \ q = \bar{q}kA\Delta s,\ \ T = \overline{T}T_{HEATER}$

The form of the differential equations is now,

(6) $\dot{\bar{q}} + \varepsilon\cdot\bar{q} = a\int_0^1 \overline{T}d\bar{s}$

(7) $\frac{\partial}{\partial\bar{t}}\overline{T} + \bar{q}\frac{\partial}{\partial\bar{s}}\overline{T} = 0$

(8) $\overline{T}_{\bar{s}=0} + \overline{T}_{\bar{s}=1} = \left(1 + \overline{T}_{\bar{s}=1}\right)\left(1 - e^{\frac{-1}{\bar{q}}}\right), \bar{q} > 0$

(9) $\overline{T}_{\bar{s}=0} + \overline{T}_{\bar{s}=1} = \left(-1 + \overline{T}_{\bar{s}=0}\right)\left(1 - e^{\frac{-1}{\bar{q}}}\right), \bar{q} < 0$

where use is made of the following dimensionless parameters,

(10) $a = \frac{g\cdot\alpha\cdot T_{HEATER}\cdot L}{2\left(k\cdot\Delta s\right)^2}$

$\varepsilon = \frac{RL}{2k\Delta s}$

Some comments should be made on equation (8) and (9). S = 0 denotes the bottom of the loop (heater) in the dimensionless coordinates, s = 1 the top (sink). In left hand side of equation (4) in dimensionless coordinates for q>0, T_{OUT} can be written as $T_{OUT} = T_{s=0+\Delta s}$, while $T_{IN} = T_{s=0-\Delta s}$. Using the anti-symmetry of the problem $T_{s=0-\Delta s} = -T_{s=1-\Delta s}$. In the limit $\Delta s \rightarrow 0$ the left hand side of (4) becomes $T_{s=0} + T_{s=1}$. Same considerations can be made when q<0.

3.1 The steady motion solution

For simplicity, coordinates without bars designate dimensionless quantities from now on. If we assume the system in steady state condition, we can consider that q and T are constant. For q>0, The equation (6) then takes the form:

$$\varepsilon \cdot q_{ss} = a \cdot T_{SS} \,. \tag{11}$$

Equation (8) takes the form:

$$2T_{SS} = (1 + T_{SS})(1 - e^{\frac{-1}{q_{SS}}}) \tag{12}$$

If T_{SS} is eliminated equations (11) and (12) finally yield the solution:

$$\frac{2q_{SS}}{\left(\frac{a}{\varepsilon}\right) + q_{SS}} = 1 - e^{-\frac{1}{q_{SS}}} \tag{13}$$

Equation (13) has one solution for a given (a/ε). The solution for selected ratios of (a/ε) is provided by Welander in table format. One can see that for a small (a/ε) q_{SS} is small, therefore T_{SS} is near to one: This implies that the temperature of the upward flow has almost the same value of the temperature of the heater. For larger values of (a/ε), q_{SS} increases, while T_{SS} decreases.

3.2 The stability of the steady motion solution

The concept which was used by Welander to analyze the stability of the solutions of the model presented in the previous section is referred to as linear stability analysis. Basically one considers small deviations in the input to the model and analyses how the deviations in the solution develop. Consider a system of differential equations (14) and its solution Y_{SOL}. Consider also a small perturbation $\vec{\varepsilon}$ of the solution. The equation for the perturbation $Y_{SOL} + \vec{\varepsilon}$, (15) can be expanded (linearized) when only small perturbations are considered. One should notice that by doing so information is lost. The results of the analysis only indicate the qualitative behavior of the solution, stable or unstable and no conclusions about the magnitude of the change can be made. If more information is wanted a non linear stability analysis should be made (examples where a non linear stability analysis was applied can be found in the papers by Suslov and Paolucci, 1999 and 1999a).

$$\dot{Y}(t) = F(Y(t)) \tag{14}$$

$$\dot{Y}_{SOL} + \dot{\vec{\varepsilon}} = F(Y_{SOL} + \vec{\varepsilon}) \approx F(Y_{SOL}) + \left.\frac{\partial F}{\partial Y}\right|_{Y_{SOL}} \cdot \vec{\varepsilon} \tag{15}$$

By using the fact that Y_{SOL} is a solution of (14) the equation (15) can be simplified to (16). This equation can be solved using the model given as eq. (17). Substituting (17) in (16) leads to the eq. (18). If any eigenvalues $Re\,\lambda_i > 0$ exist the perturbation will grow in time and the solution is unstable.

$$\dot{\vec{\varepsilon}} = \left.\frac{\partial F}{\partial Y}\right|_{Y_{SOL}} \cdot \vec{\varepsilon} \tag{16}$$

$$\vec{\varepsilon} = \vec{\xi}_i e^{\lambda_i \cdot t} \tag{17}$$

$$\left(1 \cdot \lambda_i - \left.\frac{\partial F}{\partial Y}\right|_{Y_{SOL}}\right)\xi_i = 0 \tag{18}$$

Welander assumed the solution $\overline{q}, \overline{T}$ with the derivatives q', T'. Then the linearized form of the differential equation looks like eqs. (19), while the boundary conditions take the form of the eqs. (20) below.

$$\begin{aligned} &\dot{q}' + \varepsilon \cdot q' = a \int_0^1 T' ds \\ &\frac{\partial}{\partial t} T' + \overline{q} \frac{\partial}{\partial s} T' = 0 \end{aligned} \tag{19}$$

$$\begin{aligned} &T'_{s=0} + m T'_{s=1} + n q' = 0 \\ &m = e^{\frac{1}{\overline{q}}} = \frac{1-\overline{T}}{1+\overline{T}} \\ &n = \frac{1+\overline{T}}{\overline{q}^2} e^{-\frac{1}{\overline{q}}} = \frac{1-\overline{T}}{\overline{q}^2} \end{aligned} \tag{20}$$

Exponential functions (21) were used to satisfy equation (20) and (19):

$$\begin{aligned} &q' = \hat{q} \cdot e^{r \cdot t} \\ &T' = \hat{T}(s) \cdot e^{r \cdot t} \end{aligned} \tag{21}$$

Substituting (21) in equation (19) and (20) leads to equations

$$\begin{aligned} &(r+\varepsilon)\hat{q} = a \int_0^1 \hat{T} ds \\ &r\hat{T} + \overline{q} \frac{d}{ds} \hat{T} = 0 \\ &\hat{T}(0) + m\hat{T}(1) + n\hat{q} = 0 \end{aligned} \tag{22}$$

The solution $\hat{T} = C\,exp(-rs/\overline{q})$ can be found from the second of the equations (22) which can be used to find, together with the first of the equations (22), a solution for $\hat{q} = Ca\overline{q} \cdot (1 - exp(-r/\overline{q}))/(r(r+\varepsilon))$. By considering the third of the equations of (22), the characteristic equation can be derived:

$$1 + m \cdot e^{\frac{-r}{\overline{q}}} + \frac{n \cdot a \cdot \overline{q}}{r(r+\varepsilon)}\left(1 - e^{\frac{-r}{\overline{q}}}\right) = 0 \tag{23}$$

By looking on the left hand side of equation one can see that no real solutions with r>0 exists, since for r>0 every term on the LHS is positive. So Welander investigated whether oscillatory unstable solutions exist, which means r is complex and Re r >0. For this investigation, the following new parameters (24) are introduced:

$$
\begin{aligned}
& r = i\omega \\
& \widetilde{a} = na/q \\
& \widetilde{\varepsilon} = \varepsilon/q \\
& \widetilde{\omega} = \omega/q
\end{aligned}
\qquad (24)
$$

In this case, the characteristic equation takes the form of eq. (25)

$$
\frac{e^{(i\widetilde{\omega})}+m}{e^{(i\widetilde{\omega})}-1}+\frac{\widetilde{a}}{i\widetilde{\omega}\left(i\widetilde{\omega}+\widetilde{\varepsilon}\right)}=0 \qquad (25)
$$

By separating equation (25) in real and imaginary part and utilizing proper algebraic relationships, Welander, 1967, the equation can be written in the form of eq. (26):

.

$$
\begin{aligned}
& \widetilde{\omega}^2+\left(\widetilde{\varepsilon}-\frac{1}{2}A\right)^2=\left(\frac{1}{2}A\right)^2 \\
& \widetilde{\varepsilon}=\left(\frac{1}{\overline{T}}\right)\widetilde{\omega}\,cot\left(\frac{1}{2}\widetilde{\omega}\right) \qquad (26) \\
& A(T)=\frac{1-\overline{T}^2}{\overline{T}^2}ln\left(\frac{1-\overline{T}}{1+\overline{T}}\right)
\end{aligned}
$$

For a given $\overline{T}$ the first equation of represents a circle with radius $\frac{1}{2}A$ in the $\widetilde{\varepsilon}/\widetilde{\omega}$ plane. The curves one and two of equation (26) are shown for two different values of $\overline{T}$ in Fig. 6.

By looking at the asymptotic behavior it is possible to construct a region of stability/instability for the parameters ε and $\overline{q}$. For large values of ε the region of stability and instability is separated by $\varepsilon \propto 4q^2$, while for large values of ε the stability margin is proportional to $\varepsilon \propto \pi^2/4$.

Welander numerically investigated the behavior of the loop in several regions of stability. The results are shown in Figs. 7 and 8. For small values of ε the flow grows steadily to a steady state value. If the value of ε is increased a little bit, some instabilities begin to show up. With a further increase a "stable" oscillatory behavior can be observed. Finally, growing oscillations in the flow rate show up with a regularly occurring inversion of the flow.

3.3 Numerical aspects of the Welander Loop

W. Ambrosini and J.C. Ferreri, 1997, investigated the effect of the truncation error on the stability of the numerical results for natural circulation of the Welander loop. One interesting result was that the region of stability changes dramatically with the length of the nodes which was chosen for the numerical calculation. In other words, if a very crude (coarse) nodalization was chosen, instabilities would not show up at all. Since the numerical treatment is not a topic of this lecture, only one figure with the major results is presented, Fig. 9 below.

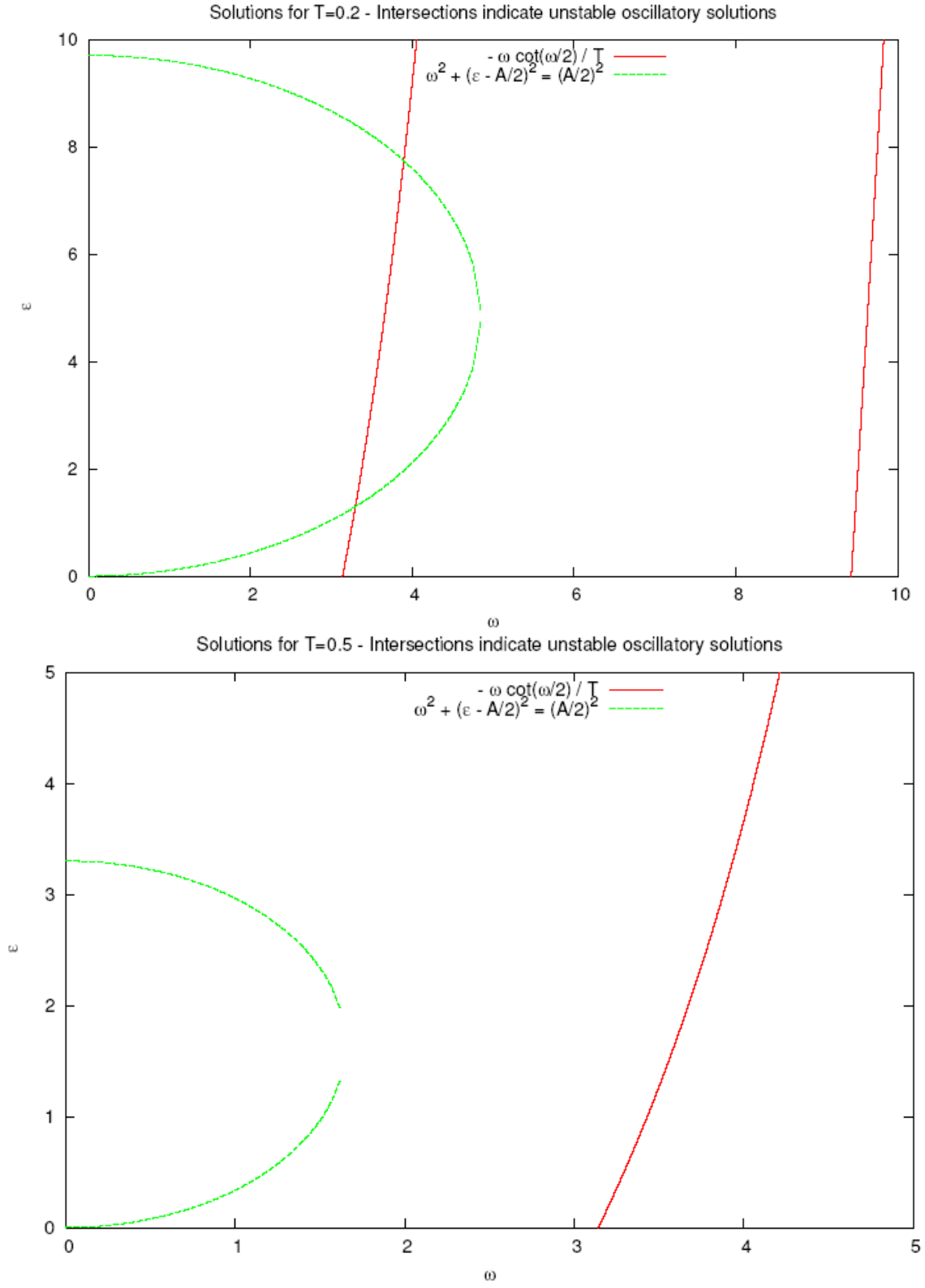

FIG. 6. Solutions to the characteristic equation for oscillatory instabilities. If the two curves intersect, the solution is oscillatory unstable. One can see that for T=0.2 the solution is oscillatory unstable, while this is not true for T=0.5(Welander, 1967).

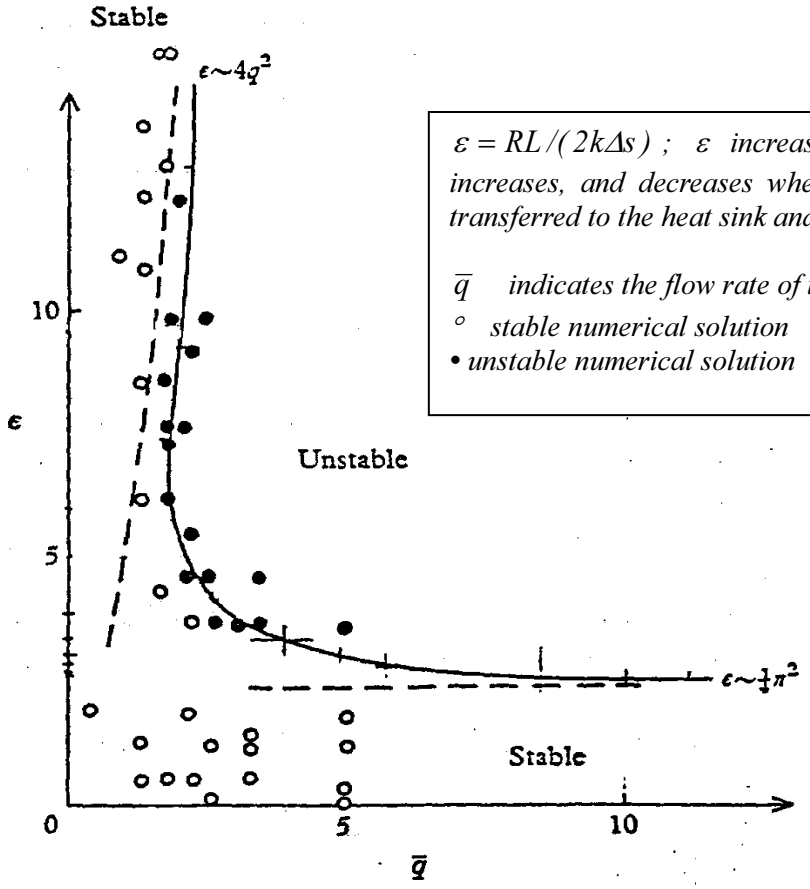

FIG. 7. Stability map calculated by Welander, 1967.

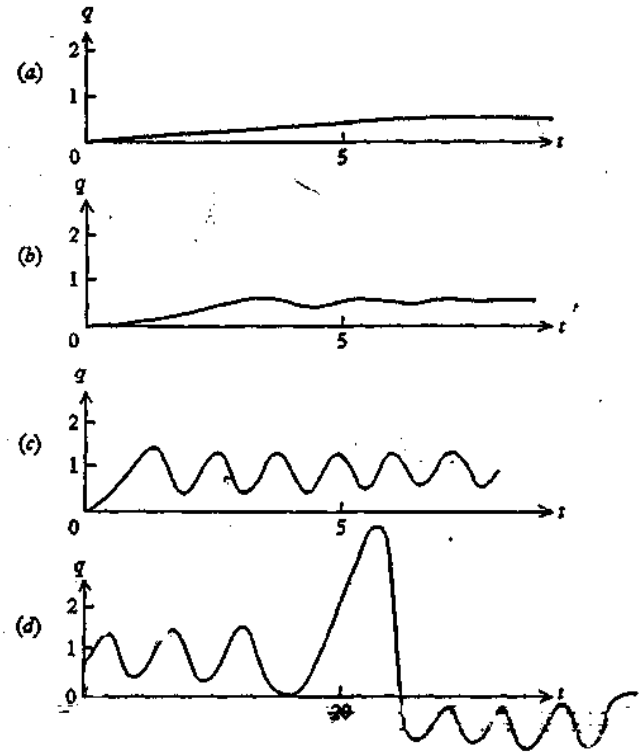

FIG. 8. Numerical solution for four cases: (a) $a = 0.4$, $\varepsilon = 0.2$ (b) $a = 2.0$, $\varepsilon = 2.0$, (c) $a = 20.0$, $\varepsilon = 20.0$ (d) $a = 40.0$, $\varepsilon = 6.0$ (Welander 1967).

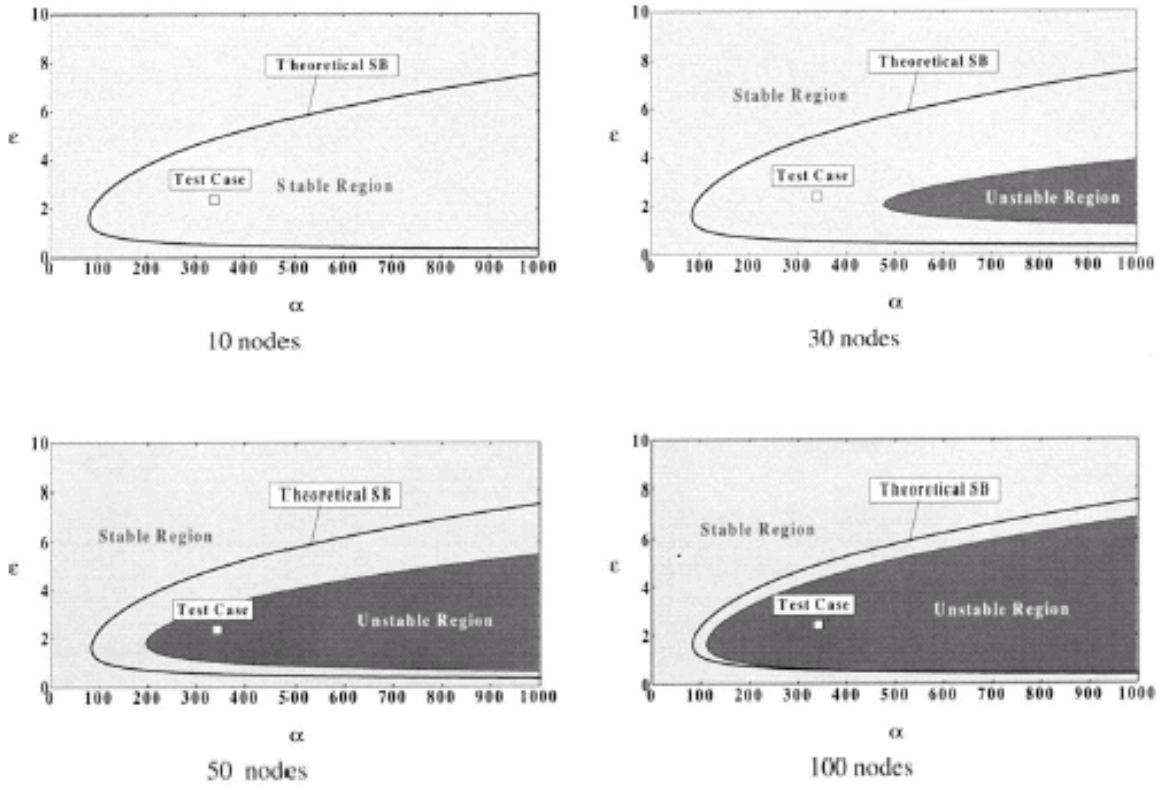

FIG. 9. Dependence of the stable and unstable region of the numerical results on the truncation error, compared to the theoretical boundary of stability (Theoretical SB). One can see the effect of the truncation error: at 10 nodes for the loop, the behavior seems stable for the whole epsilon/alpha plane. Only a nodalization with 100 nodes seems to adequately describe the problem. "Test case" refers to the selected case in the paper (Ambrosini and Ferreri, 1997).

4. THE TWO PHASE STABILITY MECHANISMS

Boiling natural circulation is a relevant cooling mechanism for the nuclear reactor systems as already mentioned. This relevance increased with the 3rd generation NPP and the studies of the 4th generation of the NPP (JPSR, AP600, SBWR, IRIS). In these reactors (i.e. AP600, IRIS, etc) the natural circulation is used for the emergency heat removal system (called "passive"), or is the major cooling mechanism (SBWR), see refs. ANS 2001 and IAEA 2005.

Flow in natural circulation system is induced by the difference of fluid density, and in two phase flow the heat input and its removal induces a large volumetric change owing to phase changes (boiling and condensation), thus the system easily becomes unstable. Flow instabilities are undesirable in boiling, condensing, and other two phase flow processes for several reasons. Sustained flow may cause forced mechanical vibration of component or system control problems, as already discussed in the case of single phase flows. Flow oscillations affect the local heat transfer characteristic and may induce boiling crisis (critical heat flux, DNB, burnout, dryout,…).

The mathematical model is based on the flow description and its boundary conditions. The flow description is based on the conservation equations (mass, momentum, energy) and the constitutive relationships that define the properties of the system with a certain degree of idealization, simplification, or empiricism. These include: the equation of state, the steam tables, the friction factor correlation, the heat transfer correlation, etc.

4.1 Structure and application of system codes

In general, the conservation principles yield three equations for each phase, plus three interface relationships. Using a six conservation equation model, such as the system codes (Relap5, Cathare2, etc…), it has been possible to take into account interfacial phenomena which result in slip and lack of thermal equilibrium, US NRC 1999. An outline of these equations is reported below in relation to one-dimensional flow inside a constant cross section duct.

The conservation equations (mass, momentum, energy) are:

$$(27)\quad \frac{\partial\left(A_k\rho_k\right)}{\partial t}+\frac{\partial\left(A_k\rho_k j_k\right)}{\partial z}=M_k$$

$$(28)\quad \frac{\partial\left(A_k\rho_k j_k\right)}{\partial t}+\frac{\partial\left(A_k\rho_k j_k^2\right)}{\partial z}+A_k\frac{\partial p}{\partial z}=-A_k\rho_k g-F_{ki}-F_{kw}$$

$$(29)\quad \frac{\partial\left(A_k\rho_k H_k\right)}{\partial t}+\frac{\partial\left(A_k\rho_k j_k h_k\right)}{\partial z}=A_k\frac{\partial p}{\partial t}-A_k j_k\frac{\partial p}{\partial z}-Q_{ki}-Q_{kw}$$

while the interfacial relations are:

$$(30)\quad \sum_k M_k=0$$

$$(31)\quad \sum_k F_{ki}=0$$

$$(32)\quad \sum_k Q_{ki}=0$$

Considering the conservation equations of the mass and the momentum it is possible to derive the slip equation for the two phases, by the elimination of the $\frac{\partial p}{\partial z}$ term, assuming: $A_k=const$, $A_g=\alpha$ and $A_l=1-\alpha$.

$$(33)\quad A_k\frac{\partial p}{\partial z}+A_k\rho_k\frac{\partial j_k}{\partial t}+A_k j_k\left(\underbrace{\frac{\partial\rho_k}{\partial t}+\rho_k\frac{\partial j_k}{\partial z}+j_k\frac{\partial\rho_k}{\partial z}}_{M_k}+\rho_k\frac{\partial j_k}{\partial z}\right)=-A_k\rho_k g-F_{ki}-F_{kw}$$

Making the difference between the two equations for the liquid and the vapor phases, the result

$$(34)\quad \begin{aligned}&\rho_l\left(\frac{\partial j_l}{\partial t}+j_l\frac{\partial j_l}{\partial z}\right)-\rho_v\left(\frac{\partial j_v}{\partial t}+j_v\frac{\partial j_v}{\partial z}\right)=\\&-\left(\rho_l-\rho_v\right)g-\left(\frac{F_{li}+j_l M}{1-\alpha}\right)+\left(\frac{F_{vi}+j_v M}{\alpha}\right)-\left(\frac{F_{iw}}{1-\alpha}-\frac{F_{vw}}{\alpha}\right)\end{aligned}$$

constitutes the so-called ‘slip equation’.

The equations (27), (28) and (29), the interfacial relations (30), (31) and (32) and the interfacial energy transfers, the interfacial momentum transfer, and the transport equation for non-condensable gas (not reported here), represent the “basic module” equations for thermal-hydraulic system codes like Relap5 (see above) and Cathare. Those time domain codes have been extensively used for the

instability analyses either in two phase conditions, e.g., D'Auria and Pellicoro, 1996, D'Auria et al., 1996, or in single phase conditions, e.g. D'Auria et al., 1999, Misale et al., 1999.

The application of system codes in single and two phase conditions shows that predictive capabilities are available to reproduce existing experimental conditions (see also D'Auria et al., 1996a, and Mori et al., 2000), see also Fig. 10 related to single phase conditions. However, the capability to predict unknown system conditions remains questionable.

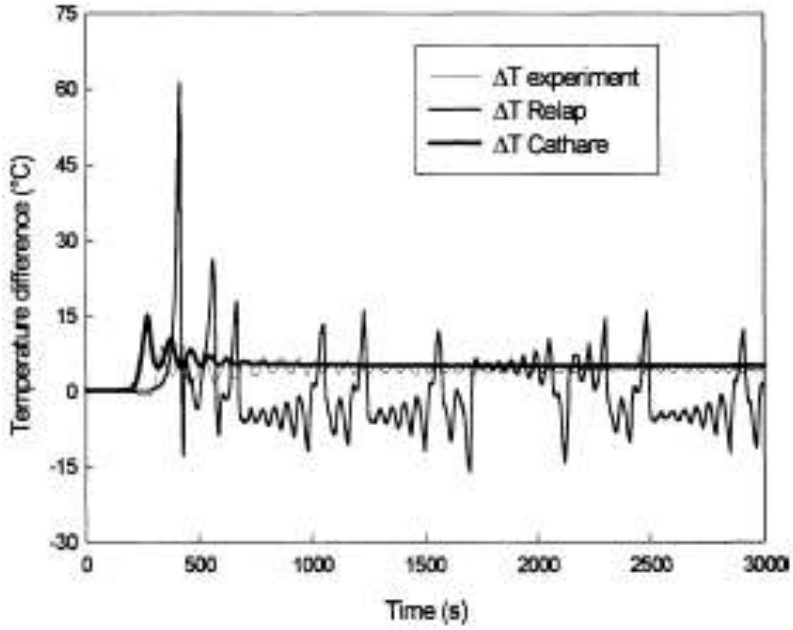

FIG. 10. Application of system codes to the prediction of stability in single phase conditions (D'Auria et al., 1996).

4.2 Structure and application of simplified models

Without entering the frequency domain codes, related details can be found in D'Auria et al. 1997, another computational approach is based upon the utilization of simplified models in order to gain physical understanding of the phenomena.

This section is focused on the work performed by W. Ambrosini et al., 1999 related to the stability of the thermo-siphon loop and in particular on the linear analyses and non-linear analyses, discussing some of the basic mechanisms involved in density wave instabilities. The considered physical model is quite simple and involves a boiling channel with constant pressure drop and inlet sub-cooling boundary conditions. An arbitrary axial distribution of heat flux is allowed and both distributed and singular pressure drop are included. Heater dynamics is modeled making use of a radial lumped heat structure model, which is axially discretized coherently with the hydraulic channel.

The two phases are assumed in thermal and mechanical equilibrium according to the HEM. In order to analyze the flow in the system, simplified equation (HEM approximation) are derived from the set of eqs. (27) to (29) with the following definitions and hypotheses:

- $A_k = const$, $A_g = \alpha$ and $A_l = 1 - \alpha$.
- The terms $\frac{\partial p}{\partial t}$ and $\frac{\partial p}{\partial z}$ are neglected in the energy equation in order to have the pressure only in momentum equation.

- $\sum_k Q_{kw} = q'''$ where q''' is the heat input per unit of volume.
- $\sum_k F_{kw} = F_{TP}$ where F_{TP} is the two phase friction pressure drop.

The equations are reduced to a set of three partial differential equations, where frictional dissipation and pressure energy are neglected.

$$\frac{\partial[\alpha\rho_v + (1-\alpha)\rho_l]}{\partial t} + \frac{\partial[\alpha\rho_v j_v + (1-\alpha)\rho_l j_l]}{\partial z} = 0 \tag{35}$$

$$\frac{\partial[\rho_l(1-\alpha)j_l + \rho_v\alpha j_v]}{\partial t} + \frac{\partial[\rho_l(1-\alpha)j_l^2 + \rho_v\alpha j_v^2]}{\partial z} + \frac{\partial p}{\partial z} + F_{lw}(1-\alpha) + F_{vw}\alpha + [\rho_l(1-\alpha) + \rho_v\alpha]g = 0 \tag{36}$$

$$\frac{\partial[\rho_l(1-\alpha)H_l + \rho_v\alpha H_v]}{\partial t} + \frac{\partial[\rho_l(1-\alpha)j_l H_l + \rho_v\alpha j_v H_v]}{\partial z} = q''' \tag{37}$$

The homogeneous equilibrium model (HEM) is characterized by the assumption that the two phase flow is an emulsion (i.e. a continuous fluid with small and evenly distributed bubbles or droplets) in thermal and mechanical equilibrium. The resulting boiling channel equations are:

$$\frac{\partial\rho}{\partial t} + \frac{\partial\rho j}{\partial z} = 0 \tag{38}$$

$$\frac{\partial\rho j}{\partial t} + \frac{\partial\rho j^2}{\partial z} + \frac{\partial p}{\partial z} = -\rho g - \left[\frac{f}{D_h} + 2K_{in}\delta_d(z) + 2K_{ex}\delta_d(z-L)\right]\frac{\rho j^2}{2} \tag{39}$$

$$\frac{\partial\rho h}{\partial t} + \frac{\partial\rho h j}{\partial z} = \begin{cases} q_0'' \dfrac{\Pi_h}{A} f_q(z) & \Rightarrow \textit{no heater} \\ \dfrac{\Pi_h}{A} H[\vartheta_H(z) - \vartheta(z)] & \Rightarrow \textit{with heater} \end{cases} \tag{40}$$

where δ_d is a dimensional Dirac's delta function [m^{-1}].

The energy equations have been written for two different situations analyzed by Ambrosini: the former considers only the imposed heat flux given to the fluid, the latter takes into account also the heat capacity of the heater.

The balance equation can be assumed in dimensionless form assuming a reference pressure to evaluate the saturated fluid properties, which are considered independent of the local value of the pressure. The main dimensionless groups useful for this analysis are able to take into account the fluid properties, the gravity, the pressure, the inlet velocity, the inlet enthalpy, and the heat flux:

- $N_{pch,}$ i.e., the phase change number involving the reciprocal flow rate versus heating power ratio and includes the specific volume ratio;
- N_{sub}, i.e. the sub-cooling number, that includes the specific volume ratio (Ishii, 1970);
- Fr, i.e. the Froude number, that represents the ratio of inertia to buoyancy (Latrofa, 2000).

The resulting dimensionless equations are

$$(41)\quad \frac{\partial \rho^*}{\partial t^*}+\frac{\partial G^*}{\partial z^*}=0$$

$$(42)\quad \frac{\partial G^*}{\partial t^*}+\frac{\partial}{\partial z^*}\left(\frac{G^{*2}}{\rho^*}\right)+\frac{\partial \rho^*}{\partial z^*}=-\frac{\rho^*}{Fr}-\left[\Lambda+K_{in}\delta^*(z^*)+K_{ex}\delta^*(z^*-1)\right]\frac{G^{*2}}{\rho^*}$$

$$(43)\quad \frac{\partial \rho^* h^*}{\partial t^*}+\frac{\partial G^* h^*}{\partial z^*}=\begin{cases} N_{pch} f_q^*(z^*) & \Rightarrow \textit{no heater} \\ K_H\left[\vartheta_H^*(z^*)-\vartheta^*(z^*)\right] & \Rightarrow \textit{with heater}\end{cases}$$

where δ^* and f_q^* are respectively a dimensionless Dirac's delta function and the heat flux distribution function.

In the case of forward flow at both the inlet and the outlet sections, constant values of dimensionless pressure in the plena and h^*_{in}=-N_{sub} and are assumed as boundary conditions for transient analysis. The boiling channel in Fig. 11 is considered that is sub-divided into N_n nodes of equal size that are connected by junctions.

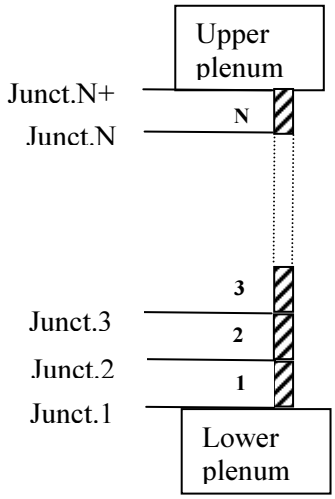

FIG. 11. Boiling channel discretization (Ambrosini et al., 1999)

Mass and energy balance equations are solved within each node and momentum equations are solved at junctions, resulting in a classical staggered mesh scheme. Conservative and non-conservative forms of balance equations are adopted in order to impose basic conservation principles and obtain an implicit treatment of the coupling between pressure and flow.

Dimensionless mass and energy balances in conservative form turn out to be:

$$(44)\quad \rho_i^{*n+1}=\rho_i^{*n}+\frac{G_i^{*n+1}-G_i^{*n}}{\Delta z^*}\Delta t^* \qquad \left(i=1,\ldots,N_{n)}\right)$$

$$(45)\quad (\rho_i^* h_i^*)^{n+1}=(\rho_i^* h_i^*)^n+\left[G_i^{*n+1}h_i^{*n}-G_{i+1}^{*n+1}h_{i+1}^{*n}\right]\frac{\Delta t^*}{\Delta z^*}+\begin{cases} N_{pch}\overline{f}_q^*(z_i^*)\Delta t^* & \Rightarrow \textit{no heater} \\ K_{Hi}\left[\vartheta_{Hi}^*-\vartheta^*(h_i^*)\right]\Delta t^* & \Rightarrow \textit{with heater}\end{cases}$$

where $\overline{f}^{*}_{q}(z^{*}_{i})$ is an appropriate average over the i-th node of the flux distribution factor and quantities $\overline{h}^{*n}_{i}$ and $\overline{h}^{*n}_{i+1}$ are the "donored" junction enthalpies.

The momentum equation is discretized in space and time in the form:

$$G^{*n+1}_{i} = G^{*n}_{i} + \left[\frac{\overline{G}^{*n^2}_{i-1}}{\rho^{*n}_{i-1}} - \frac{\overline{G}^{*n^2}_{i}}{\rho^{*n}_{i}}\right]\frac{\Delta t^{*}}{\Delta z^{*}} - \frac{1}{2}\left[\rho^{*n}_{i-1} + \rho^{*n}_{i}\right]\frac{\Delta t^{*}}{Fr}$$
$$- \left[\Lambda + K_{in}\hat{\delta}^{*}(z^{*}_{i}) + K_{ex}\hat{\delta}^{*}(z^{*}-1)\right]\frac{2\left|G^{*n}_{i}\right|G^{*n+1}_{i}}{\rho^{*n}_{i-1}\rho^{*n}_{i}}\Delta t^{*} + \left(p^{*n+1}_{i-1} - p^{*n+1}_{i}\right)\frac{\Delta t^{*}}{\Delta z^{*}} \qquad (i = 1,\ldots,N_{n}+1) \tag{46}$$

where $\hat{\delta}^{*}$ is a Dirac's delta function operating over a discretized domain and $\overline{G}^{*n}_{i-1}$ and $\overline{G}^{*n}_{i}$ are node average mass fluxes. When the heater dynamics is taken into consideration, the following dimensionless equations are solved in closed form to provide the new time step values of heater temperature:

$$N_{MH}\frac{d\vartheta^{*}_{Hi}}{dt^{*}} = N_{pch}\overline{f}_{q}\left(z^{*}_{i}\right) - K_{Hi}\left[\vartheta^{*}_{Hi} - \vartheta^{*}\left(h^{*}_{i}\right)\right] \qquad \left(i = 1,\ldots,N_{n)}\right) \tag{47}$$

Once the heat input to the channel nodes is known (with or without heater dynamics), linearized (non-conservative) forms of mass and energy balance equations and the momentum balance equations are combined resulting in a three point standard algorithm. Momentum equations is then used again to update dimensionless function mass fluxes on the basis of the new time step dimensionless nodal pressures; mass and energy balances in conservative form are then used to evaluate ρ^{*n+1}_{i} and h^{*n+1}_{i}.

To solve the ambiguity in the definition of nodal density as calculated by mass balance, the state relationship value of the nodal dimensionless density at the new time-step is assumed equal to the one corresponding to the new dimensionless enthalpy, as it is justified by the fact that the mass error at each time step is very small.

For each assigned set of dimensionless parameters, steady-state conditions are calculated at constant dimensionless inlet mass flux, providing initialization of channel nodal variables and the value of the overall pressure drop across the channel to be imposed as a constant boundary condition during the analysis. An impulse perturbation in the outlet pressure is used to start system oscillation.

In order to provide information about the linear stability of the boiling channel, the obtained discretized equations are then linearized by perturbation. This approach adopted by Ambrosini 2001 is based on the simple matrix formulation that relates the vectors of the system state variables at two subsequent time steps:

$$(\delta y)^{n+1} = -\left(J^{s}_{y^{n+1}}\right)^{-1}J^{s}_{y^{n}}(\delta y)^{n} = A(\delta y)^{n} \tag{48}$$

where $J^{s}_{y^{n+1}}$ and $J^{s}_{y^{n}}$ are the Jacobian matrices of the non-linear discretized equations with respect to y^{n} and y^{n+1}. Considering the eigenvalues ($\lambda_{i} \in C$) of the matrix A, the criterion $\rho(A) = \left|\lambda_{\max}\right| > 1$ is the condition for the asymptotic instability.

The quantities

$$(49)\quad z_R = \mathrm{Re}(\lambda_{\max}) = \frac{\ln[\rho(A)]}{\Delta t^*} \qquad z_I = \mathrm{Im}(\lambda_{\max}) = \frac{1}{\Delta t^*} ar\cos\frac{\mathrm{Re}(\lambda_{\max})}{\rho(A)}$$

are useful in studying stability of small perturbation. They represent respectively a measure of the amplification ($Z_R<0$) or damping ($Z_R>0$). The period (T) and the decay ratio (DR) of the oscillations are:

$$(50)\quad T_{fast} = \frac{2\pi}{z_I} \qquad DR = e^{\frac{2\pi z_R}{z_I}}$$

The "stability plane" is the N_{sub} versus N_{pch} plane, Fig. 12, and the stability is studied in the regions in which $Z_R>0$.

The figure concerns the Ambrosini's analyses, where two cases are analyzed. These differ for the Froude number and for the friction parameters. In particular: the case (a) regards a vertical channel (Fr=0.033) characterized by $\frac{fl}{2D_h}$=2.85 and the case (b) regards a nearly horizontal channel (Fr=10^5) characterized by $\frac{fl}{2D_h}$= 0.

The figures show the shape of the neutral stability, the expected separation between the density-wave and the Ledinegg (excursive) instability regions. Furthermore, the system condition $N_{pch} > N_{sub}$, corresponds to a positive exit thermodynamic quality and the system is 'less stable' than in the single phase region.

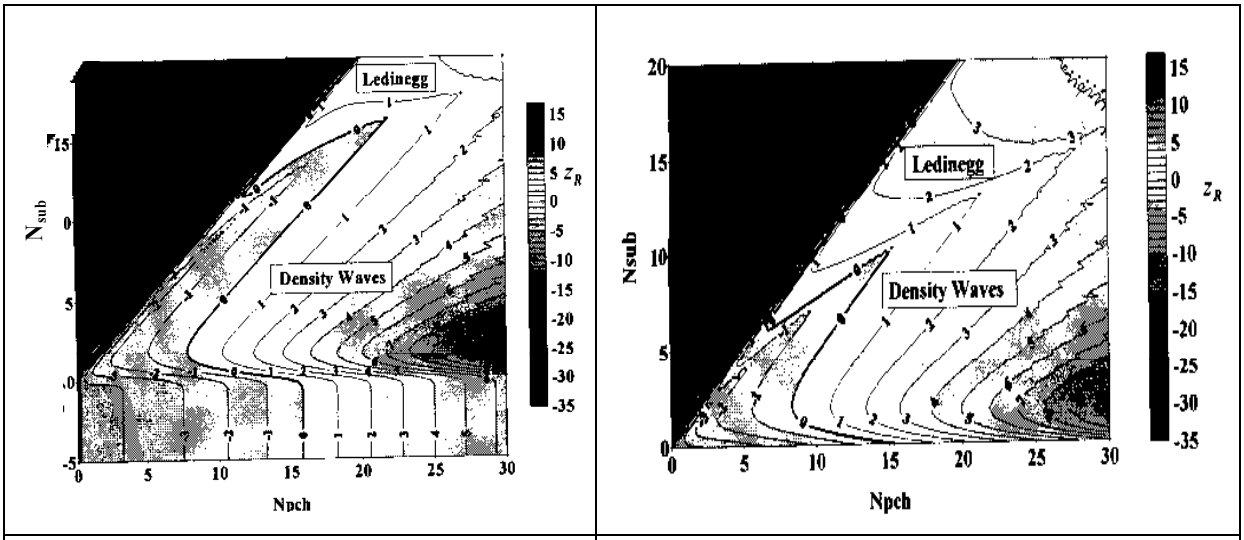

(a) (b)

FIG. 12. Stability map obtained by a HEM type model (Ambrosini, 2001)

5. SUMMARY AND CONCLUSIONS

A non systematic overview of instabilities in single and two phase fluid-dynamic systems has been given. The attention is focused on measured data from complex (e.g. BWR) and simple (e.g. NC loop) systems in either single and two-phase flow conditions. Furthermore the bases of the analytical tool in the time domain that are suited for stability analysis are presented together with selected-significant results from the application.

The overview is expected to stimulate the curiosity of the reader to learn more and more on this subject, also considering the referenced papers and documents.

NOMENCLATURE

Roman letter

A	Cross sectional area [m^2]
B	buoyancy force [N]
D_h	hydraulic diameter [m]
f	friction factor
f_q	power distribution factor
F	momentum losses and friction force [N]
$Fr = w_0^2 / gl$	Froude number
g	gravity [m/s^2]
G	mass flux [$kg/(m^2s)$]
$G^* = \rho^* j^*$	dimensionless mass flux
h	specific enthalpy [J/kg]
$h^* = \frac{h - h_f}{h_{fg}} \frac{v_{fg}}{v_f}$	dimensionless enthalpy
H	heat transfer coefficient [$W/(m^2K)$]
j	volumetric flux [m/s]
$j^* = j / w_0$	dimensionless volumetric flux
$K_{in,ex}$	singular pressure drop coefficient
$K_H = \frac{H \Pi_h L}{w_0 A c_{pf} \rho_f}$	dimensionless heat transfer coefficient
L	length [m]
$N_{MH} = \frac{M_h c_{pH}}{LA \rho_f c_{pf}}$	heater capacity number
$N_{pch} = \frac{q_0'' \Pi_h L}{\rho_f w_0 h_{fg} A} \frac{v_{fg}}{v_f}$	phase change number
$N_{sub} = \frac{h_f - h_{in}}{h_{fg}} \frac{v_{fg}}{v_f}$	sub-cooling number
N_n	number of nodes
p	pressure [kg/s^2m]

$p^* = p / \rho_f w_0^2$	dimensionless pressure
q	flow rate [kg/m^2]
q''	heat flux [W/m^3]
Q	heat transfer per unit time and volume
R	frictional coefficient [s^{-1}]
t	time [s]
$t^* = tw_0 / L$	dimensionless time
v	specific volume [m^3/kg]
z	axial coordinate [m]
$z^* = z / L$	dimensionless axial coordinate

Greek letter

α	thermal expansion coefficient [m]
Π_h	heated perimeter [m]
ϑ	temperature [K]
$\vartheta^* = \begin{cases} h^* \; if \; h < 0 \\ 0 \; if \; h \geq 0 \end{cases}$	dimensionless fluid temperature
ϑ_h^*	dimensionless heater temperature
Λ	friction perimeter
ρ	density [kg/m3]
$\rho^* = \rho / \rho_f$	dimensionless density

Subscripts

f	liquid phase
fg	difference between vapour and liquid
g	vapour phase
in	inlet
ex	exit
0	reference value

Superscripts

H	heater
i	i-th node or junction
n	n-th time level
n+1	(n+1)-th time level
•	dimensionless value
T	transposed

ACKNOWLEDGEMENT

The authors wish to acknowledge the support given by B. Neykov during the development of this work. The updated version of the paper has been prepared within the framework of an IAEA grant and J. Cleveland is acknowledged.

REFERENCES

W. Ambrosini, F. D'Auria, A. Giglioli, 1995, Coupled Thermal-Hydraulic and Neutronic Instabilities in the LaSalle-2 BWR Plant, *XIII Congresso Nazionale sulla Trasmissione del Calore dell'Unione Italiana di Termofluidodinamica – UIT, Bologna, Italy.*

W. Ambrosini, J.C. Ferreri, 1997, The effect of truncation error on the numerical prediction of linear stability boundaries in a natural circulation single-phase loop, *Nuclear Engineering and Design*, **Vol. 183**, pp. 53-76.

W. Ambrosini, P. Di Marco, A. Susanek, 1999, Prediction of Boiling Channel Stability by a Finite – Difference Numerical Method, *2nd International Symposium on Two Phase Flow Modelling and Experimentation*, Pisa, Italy.

W. Ambrosini, 2001, On Some Physical and Numerical Aspects in Computational Modelling of One-Dimensional Flow Dynamics, *7th International Seminar on Recent Advances in Fluid Mechanics, Physics of Fluids and Associated Complex Systems, Buenos Aires, Argentina.*

W. Ambrosini, A. Del Nevo, F. Oriolo, 2004, *Thermal-Hydraulic Stability Analyses in IRIS Helical Coil Steam Generators with the Relap5 Code*, DIMNP Internal Report, Pisa.

ANS, Technical Working Group1 – Advanced Water Cooled Reactors, 2001, Generation IV Water Cooled Reactor Concepts, Generation IV Roadmap Session, *ANS Winter Meeting Reno, NV.*

J. A. Boure, A. E. Bergles, 1973, L. S. Tong, *Review of Two Phase Flow Instability*, Nuclear Engineering and Design, North-Holland Publishing Company.

P. Carey, 1992, *Liquid-Vapor Phase Change Phenomena*, Taylor & Francis.

J.D. Crowley, C. Deanne and S.W. Gouse Jr., 1969, Two Phase Oscillations in Vertical, Parallel, Heated Channels, *Proc. Symp. on Two Phase Flow Dynamics, Commission of the European Communities, Brussels, pp. 1131-1172.*

F. D'Auria, V. Pellicoro, 1996, Local Instability in BWR Reactor Simulator, *Int. Conf. on Nuclear Engineering (ICONE-4), Vol. 3, pp. 157-, New Orleans U.S.A*.

F. D'Auria, V. Pellicoro, O. Feldmann, 1996, Use of Relap5 Code to evaluate the BoP influence following instability events in BWR, *Int. Conf. on Nuclear Engineering (ICONE-4), Vol. 3, pp. 71-, New Orleans, USA*

D'Auria F., Frogheri M., Galassi G.M., 1996a, Participation to OECD/NEA BWR Benchmark with Relap5/mod2 code, *Int. Conf. Nuclear Option in Countries with Small and Medium Electricity Grid, Opatjia (HR), Oct. 7-9.*

F. D'Auria (Editor), W. Ambrosini, T. Anegawa, J. Blomstrand, J. In De Betou, S. Langenbuch, T. Lefvert, K. Valtonen, 1997, State of the Art Report on Boiling Water Reactor Stability (SOAR ON BWRS), *OECD-CSNI Report OECD/GD (97) 13, Paris (F)*

F. D'Auria, M. Frogheri, M. Misale M., 1997a, System codes capabilities in predicting instabilities in single phase natural circulation, *4th Regional Meet. Nuclear Energy in Central Europe, Bled (SLO), Sept. 7-10.*

F. D'Auria, E. Fontani, M. Frogheri, M. Misale, A. Garcia, 1999, Analysis of single phase natural circulation experiment with Cathare V1.3U and Relap5/Mod3.2 codes, *Int. J. of Thermal Science, Vol. **38**, pages 977-983*

M. Frogheri, M. Misale, A. Oliveri, F. D'Auria F., 1998, Multidimensional aspects in single phase natural circulation, *16th Conf. of Italian Society of Heat Transport, Siena (I), June 18-19 1998.*

S. Guanghui, et. al., 2001, Theoretical Study on Density Wave Oscillation of Two Phase Natural Circulation under Low Quality Conditions, *Journal of Nuclear Science and Technology*.

IAEA, 2005, Natural Circulation in Water Cooled Nuclear Power Plants, *IAEA Tecdoc 1474, Vienna (A), pp 1-637.*

M. Ishii, N. Zuber; 1970, Thermally Induced Flow Instabilities in Two Phase Mixtures, *4th Int. Heat Transfer Conference*, Paris, Italy.

M. Ishii, 1976, *Study on Flow Instabilities in Two Phase Mixtures*, ANL-76-23.

J. Jafari, F. D'Auria, H. Kazeminejad, H. Davilu, 2003, Reliability evaluation of a natural circulation system, *Nuclear Engineering and Design*, **Vol. 224**, pp. 79-104.

S. Kakac, and H.T. Liu, 1991, Two-Phase Flow Dynamic Instabilities in Boiling Systems, *In Multiphase Flow and Heat Transfer - Second International Symposium, Washington DC, Vol. 1, pp. 403 - 444.*

E. Latrofa, 2000, Fisica Tecnica – Termodinamica, *A. Vallerini Editrice, Pisa, Italia*

M. Misale, M. Frogheri, F. D'Auria, 1999, Experiments in natural circulation: influence of scale factor on the stability behavior, *Proceeding of Eurotherm Seminar No 63, Genoa, Italy, 6-8 September, Vol. 1, pp. 109-116.*

M. Misale, P. Ruffino, M. Frogheri, 1999, The Influence of the Wall Thermal Capacity and Axial Conduction Over a Single-Phase Natural Circulation Loop: 2-D Numerical Study, *Proceeding of Eurotherm Seminar No 63, Genoa, Italy, 6-8 September, pp.177-187*.

M. Mori, F. D'Auria, W.J.M. de Kruijf, T.H.J.J. van der Hagen, 2000, Determination of BWR stability characteristics from numerically obtained system responses, *Int. Conf. Nuclear Option in Countries with Small and Medium Electricity Grids, Dubrovnik (HR), June 19-22.*

A. Petruzzi, F. D'Auria, M. Misale, 2001, Sensitivity analysis on the stability of the natural circulation in a thermo-siphon loop, *19th Conf. of Italian Society of Heat Transport, Modena (I), June 25-27.*

A. Petruzzi, F. D'Auria, M. Misale, 2002, Single phase natural circulation in a Rectangular Loop in Micro-gravity condition Space, *Technology and Application International Forum – STAIF 2002 Albuquerque (NM, USA) Feb. 4-7, American Institute of Physics 0-7354-0052-0-02.*

S.A. Suslov, S. Paolucci, 1999, Nonlinear stability of mixed convection flow under non-Boussinesq conditions. Analysis and bifurcations, *Journal of Fluid Mechanics*, **Vol. 398**, pp61-108

S.A. Suslov, S. Paolucci, 1999a, Mean flow characteristics, *Journal of Fluid Mechanics*, **Vol. 398**, pp 61-108.

US NRC 1999, RELAP5/MOD3 – Volume I - Code Structure, System Models, and Solution Methods, *Thermal Hydraulics Group; NUREG/CR-5535,Scientech, Inc.; Rockville, Maryland; Idaho Falls, Idaho, USA*.

P.K. Vijayan, H. Austregesilo, 1994, Scaling Laws for the Single Phase Natural Circulation Loops, *Nuclear Engineering and Design*, **Vol. 152**, 331-340.

P. Welander, 1967, On the oscillatory instability of a differentially heated fluid loop, *Journal of Fluid Mechanics*, **Vol. 29**, part 1, pp. 17-30.

G. Yadigaroglu and K.C. Chan, 1979, Analysis of flow instabilities, *Proceedings of the Japan–US Seminar on Two-Phase Flow Dynamics July 31–August 3, 1979, Kobe, Japan.*.